Free-Radical Scavenger Edaravone Treatment Confers Neuroprotection Against Traumatic Brain Injury in Rats

Guo-Hua Wang,[1,2] Zheng-Lin Jiang,[1] Yong-Cai Li,[3] Xia Li,[1] Hong Shi,[2] Yan-Qin Gao,[2] Peter S. Vosler,[4] and Jun Chen[2,4]

Abstract

Traumatic brain injury (TBI) is one of the leading causes of neurological disability in young adults. Edaravone, a novel synthetic small-molecule free-radical scavenger, has been shown to have a neuroprotective effect in both animal models of cerebral ischemia and stroke patients; however, the underlying mechanism is poorly understood. In this report, we investigated the potential mechanisms of edaravone treatment in a rat model of TBI. TBI was induced in the right cerebral cortex of male adult rats using Feeney's weight-drop method. Edaravone (0.75, 1.5, or 3 mg/kg) or vehicle (normal saline) was intravenously administered at 2 and 12 h after TBI. Edaravone treatment significantly decreased hippocampal CA3 neuron loss, reduced oxidative stress, and decreased neuronal programmed cell death compared to vehicle treatment. The protective effects of edaravone treatment were also related to the pathology of TBI on non-neuronal cells, as edaravone decreased astrocyte and glial activation. Lastly, edaravone treatment significantly reduced the presence of inflammatory cytokines, cerebral edema, blood–brain barrier (BBB) permeability, and, importantly, neurological deficits following TBI. Our results suggest that edaravone exerts a neuroprotective effect in the rat model of TBI. The likely mechanism is via inhibiting oxidative stress, leading to a decreased inflammatory response and glial activation, and thereby reducing neuronal death and improving neurological function.

Key words: edaravone; inflammatory cytokines; neuroprotection; oxidative stress; TBI

Introduction

Traumatic brain injury (TBI) represents a major public health problem and is the leading cause of neurological disability in young adults (Aarabi and Simard, 2009; Chua et al., 2007). Unfortunately, there are no available neuroprotective strategies to date, despite the large amount of work done in this area (Aarabi and Simard, 2009; Chew and Zafonte, 2009). Complicating factors include the pathophysiology of TBI, which involves an initial tissue loss induced directly by mechanical trauma (Maas et al., 2008), and the subsequent cascade of events such as excitotoxicity, brain edema, blood–brain barrier (BBB) disruption, programmed cell death (PCD), and pro-inflammatory reactions that trigger secondary brain damage and ultimately long-term neurological deficits (Greve and Zink, 2009; Shlosberg et al., 2010). Prevention and treatment of these secondary brain injuries are putative targets for pharmaceutical neuroprotection and represent the major framework for the therapeutic management of TBI (Besson, 2009; Chew and Zafonte, 2009).

There are multiple mechanisms underlying secondary brain damage following TBI (Stoica and Faden, 2010). Oxidative stress, secondary to excitotoxicity and intracellular calcium dysregulation, plays a central role in secondary brain neuronal death, and contributes to many of the aforementioned pathophysiological changes (Petronilho et al., 2010; Vosler et al., 2009). Oxidative stress occurs when there is an imbalance between cellular production of free radicals and the intrinsic ability of cells to sequester and eliminate these free radicals (Gilgun-Sherki et al., 2002). It begins immediately after TBI and initiates the cascade resulting in neuronal dysfunction and death, and thus plays a major role in the morbidity and mortality following TBI (Merenda et al., 2008). Importantly, enhancement of cellular defense mechanisms through the use of exogenous antioxidants is known to be neuroprotective in animal models of cerebral ischemia (Clausen et al., 2004).

[1]Department of Neuropharmacology, Institute of Nautical Medicine, Nantong University, Nantong, Jiangsu, China.
[2]State Key Laboratory of Medical Neurobiology, Fudan University, Shanghai, China.
[3]Department of Neurosurgery, People's Hospital of Ningxia, Yinchuan, Ningxia, China.
[4]Center of Cerebrovascular Disease Research, University of Pittsburgh School of Medicine, Pittsburgh, Pennsylvania.

The majority of TBI research has focused on the direct protection of neuronal cells; however, recent work suggests that non-neuronal brain cells, especially astrocytes (the predominant cell type in the human brain), may exert an active role in the pathogenesis of TBI (Laird et al., 2008). Reactive astrocytes may contribute to increased oxidative stress, inflammation, development of cerebral edema, and elevated intracranial pressure, thus exacerbating secondary brain injury following neurotrauma (Serrano-Perez et al., 2011). The contribution of reactive astrocytes to secondary injury following TBI is a relatively unexplored area of research and provides an additional therapeutic target for limiting neurological injury (Laird et al., 2008).

Edaravone (3-methyl-1-phenyl-2-pyrazolin-5-one, MCI-186) is a novel synthetic small-molecule free-radical scavenger that is neuroprotective in animal models of cerebral ischemia and currently is being used clinically in Japan to treat stroke patients (Kikuchi et al., 2010; Naritomi et al., 2010). Although additional clinical studies are necessary to verify its efficacy for ischemic stroke patients (Lapchak, 2010), edaravone's scavenging properties may make it a good candidate for TBI treatment because of the role of oxidative stress in the pathophysiology of TBI (Petronilho et al., 2010). Recently, edaravone has been tested for its neuroprotective and antioxidative effects on the brain after TBI both in rat models and in patients (Dohi et al., 2006; Dohi et al., 2007; Itoh et al., 2010). However, because many uncertainties remain about the clinical efficacy of edaravone in the treatment of TBI patients, more fundamental animal experiments are needed. This study was conducted to investigate the potential benefits of the antioxidant edaravone in a rat model of TBI with a focus on elucidating its underlying neuroprotective mechanisms.

Methods

Animals

Male Sprague–Dawley rats (SD, 250–280 g body weight) were provided by the Experimental Animal Center of Nantong University, Nantong, China. The rats were housed in a temperature- and humidity-controlled animal facility with a 12 h light/dark cycle. All procedures used in this study were in accordance with our institutional guidelines, which comply with internationally accepted humane standards.

TBI

Rats were anesthetized using 2 mL enflurane in an ether jar, and maintained with 10% chloral hydrate (400 mg·kg^{-1}, i.p.). The head of the animal was fixed with a stereotactic frame. A right parietal craniotomy (3.5 mm posterior and 2.5 mm lateral to bregma, diameter 5 mm) was conducted with a drill, under aseptic conditions. Following Feeney's weight-drop model with slight modifications (Wang et al., 2010), a standardized parietal contusion was reproduced by dropping a 20 g, flat-ended steel rod (diameter 4.5 mm) from a height of 30 cm onto a piston resting on the dura. The piston was allowed to compress the brain tissue at a depth of 2.5 mm. Heart rate, arterial blood pressure, and rectal temperature were monitored. Animal temperature was maintained at 37 ± 0.5°C throughout the experiment. Sham-operated rats were anesthetized, and only the right parietal craniotomy was performed. All animals were randomly distributed into the corresponding groups. Of note, all measurements were taken 72 h after TBI, to allow for multiple measurements within rats, to decrease the total number of rats killed for the current study.

Drug application

Edaravone (Simcere Pharmaceutical Group, Nanjing, China) was injected via vena caudalis at 2 h after TBI and repeated 10 h later. To observe the dose-dependent effect, rats were injected with 0.75 mg, 1.5 mg, or 3 mg (kg^{-1}) of edaravone, respectively. These doses correspond to the most commonly used dose in clinical trials, 30 mg i.v., b.i.d. (Lapchak, 2010), by implementing the body surface normalization method to extrapolate from humans to rats (Regan-Shaw et al., 2008). The 10 h interval between edaravone doses was implemented to correspond to the b.i.d use in clinical trials (Lapchak, 2010). The vehicle group was treated with normal saline. Edaravone was used at 1.5 mg·kg^{-1} in other observations including assays of oxidative stress, enzyme-linked immunosorbent assay (ELISA), immunohistochemistry, and immunofluorescence staining, based on our results.

Nissl staining and immunohistochemistry

Three days after TBI, animals were killed with deep anesthesia, by perfusion through the left ventricle with 200 mL of ice-cold phosphate-buffered saline (PBS, 0.1 mol/L), followed by 400 mL of 4% paraformaldehyde in 0.1 mol/L PBS (pH 7.4). Rat brains were then removed and postfixed for 24 h in the same fixative. The postfixed brains were dry-protected in 30% sucrose in PBS. The brain tissue was coronally sectioned (20 μm thick) with a cryostat (CM1900, Leica, Bensheim, Germany). Sections between 3 and 4.5 mm posterior to bregma were selected. The free-floating sections were prepared for double immunostaining. Alternate sections were treated with Nissl staining for histological assessment of damage, and the adjacent section was processed for immunohistochemical analysis.

For Nissl staining, the free-floating sections were mounted onto slides and processed through different baths in the following order: chloroform, 30 min; acetone, 15 min; 100% ethyl alcohol (EtOH), 30 sec; 95% EtOH, 30 sec; 70% EtOH, 30 sec; distilled water, 30 sec, twice; cresyl violet, 20 min; distilled water, 30 sec, three times; 70% EtOH, 1 min; 95% EtOH, 1 min; 100% EtOH, 1 min; chloroform, 5 min; differentiator (95% EtOH, with glacial acetic acid added to reach a pH of 4.1), 6 min; 95% EtOH, 2 min, 100% EtOH, 3 min, twice; xylene, 2 min; xylene, 3 min, twice. After staining, sections were mounted with neutral balata and covered with a cover-slip. The brain slices in each section were photographed (DM5000B, Leica, Bensheim, Germany). Normal neuronal profiles in the pyramidal cell layer of hippocampal area CA3 on the right side, which were taken from three sections in the different coronal levels (3.1, 3.8, and 4.4 mm posterior to bregma) per hemisphere, were counted. In each section, the number of neuronal profiles, identified as having a distinct nucleolus, was assessed under a microscopic field in a 1-mm length of the CA3 area at $\times 200$. The neuronal number of each animal was represented as the average of three sections ($n = 6$ rats per group).

Immunohistochemical stains for light microscopy were performed using antibodies for the following proteins: glial

fibrillary acidic protein (GFAP, 1:200 monoclonal mouse-anti-GFAP, ThermoFisher Scientific, Waltham, MA), vimentin (1:100 monoclonal mouse-anti-vimentin, ThermoFisher Scientific), S-100 (1:200 monoclonal mouse-anti-S-100, Chemicon, Billerica, MA), OX42 (1:200 monoclonal mouse-anti-S-100, Chemicon) and activated caspase-3 (1:100 polyclonal rabbit anti-cleaved caspase-3 [Asp175], Bioworld Technology Inc., Louis Park, MN). Endogenous peroxidase was blocked with 0.3% H_2O_2 in methanol and was followed by incubation in blocking buffer (10% normal goat serum and 0.3% Triton-X in TBS) for 30 min. The primary antibodies were diluted in commercial antibody diluent (Beyotime, Jiangsu, China), and sections were incubated overnight at 4°C. Immuno-reactions were visualized using the ABC kit (Zhongshan Biotechnology Company, Beijing, China) for GFAP, vimentin, S-100, and caspase-3. Labeling was visualized using 3,3′-diaminobenzidine-tetrahydrochloride (DAB, Zhongshan Biotechnology Company). Immunofluorescence was visualized using fluorescent secondary antibodies (1:200 anti-Mouse TRITC or 1:200 anti-Rabbit TRITC, Sigma-Aldrich Corporation, CN: T5393 and T5268, respectively). Sections were evaluated under light or fluorescent microscopes (DM5000B, Leica, Bensheim, Germany) as appropriate. Simultaneously, a negative control was performed with tissue incubated without primary antibody. To obtain standardized results from all animals, evaluations of pathology were performed from six sections per hemisphere with two sections from each different coronal level (3.1, 3.8, and 4.4 mm posterior to bregma). GFAP-, vimentin- and S100-positive astrocytes were counted in the brain cortex surrounding the primary injury under ×200 optical fields using a 610- ×610- μm (0.3721 mm^2) prefrontal grid.

Detection of free radicals

Rats were killed at 72 h after TBI, and the brains were immediately removed. The surrounding brain tissue of the injured cortex was dissected on ice from the region that was <3 mm from the margin of the contusion site. A portion of tissue (0.5 g) was homogenized (4.5 mL of 0.86% cold physiological saline) on ice using a glass homogenizer, and then the supernatant was collected after centrifuging at 4°C and $4000 \times g$ for 15 min. Neurochemical assays were conducted in accordance with the manufacturer's instructions for commercial kits of superoxide dismutase (SOD), malondialdehyde (MDA), nitric oxide (NO) and inducible nitric oxide synthase (iNOS) assays, which were purchased from the Nanjing Jiancheng Bioengineering Institute (Nanjing, China).

Electron microscopy

For electron microscopy, 72 h after TBI, deeply anesthetized rats were perfused with saline followed by cold fixative containing 4% paraformaldehyde, 0.1% glutaraldehyde in 0.1 mol/L PBS (pH = 7.4). The brain tissue surrounding the cortical contusion site (Fig. 2A) was dissected under a microscope into ~1-mm tissue blocks and postfixed with 2% glutaraldehyde for 24 h. Samples were then rinsed in PBS and fixed with osmium tetroxide, dehydrated in a graded series of acetone, embedded in epon-araldite epoxy resin, sectioned at 60 nm, and examined with a JEM-1230 (JEOL, Tokyo, Japan) transmission electron microscope.

Western blot analysis

At 72 h after TBI, each rat was decapitated under 10% chloral hydrate anesthesia. The peripheral cortex surrounding the contusion site (Fig. 2A) was harvested under a stereotaxic device (Stoelting Co., Wood Dale, IL) for assay of the expression of activated caspase-3, GFAP, vimentin, and S-100. The brain tissue was homogenized in an ice-cold buffer (tris-[hydroxymethyl] aminomethane 50 mM, pH 7.4; NaCl 150 mM; 0.5% Triton X-100; edetic acid 1 mM; phenylmethylsulfonyl fluoride 1 M; and aprotinin 5 mg·L^{-1}), and centrifuged at $14,000 \times g$ at 4°C for 30 min. The supernatants were then collected and total protein was determined by bicinchoninic acid assay (Beyotime Biotechnology, China). Equal protein concentrations were electrophoresed through a 15% sodium dodecyl sulfate polyacrylamide gel, and electrically transferred to a nitrocellulose membrane. This membrane was incubated at 4°C overnight in tris-(hydroxymethyl)-aminomethane buffered saline (TBS) containing 5% milk, and detected with the primary antibody against cleaved caspase-3, GFAP, vimentin, and S-100 (at 1:200 dilutions). After washing with TBS, the membranes were incubated with the secondary antibodies (horseradish peroxidase-conjugated goat anti-rabbit and anti-mouse IgG, Pierce Biotechnology Inc., Rockford, IL) at room temperature for 1 h. Membranes were scanned and quantified by Scion Image (Scion, Frederick, MD), and the amount was normalized to β-actin values in the same lane.

ELISA

Measurements of interleukin-6 (IL-6), tumor necrosis factor α (TNF-α), interleukin-1β (IL-1β), and interleukin-10 (IL-10) in the brain samples were performed using ELISA 3 days after TBI. Eighteen rats ($n = 6$ for each group) were used for detection. The frozen brain tissue (0.1 g) was homogenized with a glass homogenizer in 1 mL buffer containing 1 mmol/L phenylmethylsulfonyl fluoride, 1 mg/L pepstatin A, 1 mg/L aprotinin, and 1 mg/L leupeptin in PBS (pH 7.2) and centrifuged at $12000 \times g$ for 20 min at 4°C. The supernatant was then collected and total protein was determined by bicinchoninic acid assay (Beyotime Biotechnology, China). The levels of IL-6, TNF-α, IL-1β, and IL-10 in the tissue supernatants were determined with ELISA assay kits (NeoBioscience Technology Co. Ltd., Beijing, China). The measurements were performed step by step based on the ELISA kit protocol booklet. Values were expressed as ng cytokine/g protein.

Gravimetric analysis of brain water content

Rats were anaesthetized with 10% chloral hydrate (400 mg/kg, i.p.) and killed by decapitation 72 h after TBI. The brains were immediately removed and separated into left and right hemispheres. After the determination of the wet weight of each hemisphere, the tissue was dried for 72 h at 100°C and measured for dry weight. Percentage of brain water content was calculated as 100×(wet weight − dry weight)/wet weight.

Determination of BBB permeability

The procedure was performed as previously described (Wang et al., 2010). At 72 h after TBI, 0.2 ml·100 g^{-1}·wt of 2.5% Evans blue solution was administered intravenously to the rats. After 2 h, the rats were perfused with 60 mL normal saline through the left ventricle. Rat brains were removed and

extracted in 3 mL formamide at room temperature for 72 h. The Evans blue dye was then quantified fluorometrically (Hitachi F-4010 fluorescence spectra photometer, EX = 625, EM = 675, slit = 18). Brain tissue was then dried for 3 days at 100°C. The content of Evans blue was expressed as micrograms per gram of dry weight of brain tissue.

Neurological evaluation

The beam-balancing test and prehensile traction test to evaluate neurological function were performed by a researcher blinded to study groups as previously described (Wang et al., 2010). A higher score represented a more severe neurological deficit. All animals were trained prior to TBI, and those with abnormal neurological function at baseline were eliminated. The final test was conducted 72 h after TBI.

Statistical analysis

All values are presented as mean ± standard deviation. Data of two groups were analyzed with Student's t test (non-directional), and data of repeated groups were analyzed with one-way ANOVA and Newman–Keuls test for post-hoc comparisons. Pearson product linear regression was used to correlate the number of CA3 neurons with neurological deficit scores, and the amounts of inflammatory cytokines with the level of SOD and MDA. Differences were considered statistically significant at a level of $p < 0.05$.

Results

Neuroprotective effect of edaravone against TBI

We initially wanted to confirm that edaravone was neuroprotective in our model. We therefore examined the dose–response effect of edaravone on overall neuronal number following TBI. Edaravone (0.75, 1.5, or 3 mg/kg) or normal saline was intravenously administered at 2 and 12 h after TBI, and all animals were killed at 72 h after TBI. The weight-dropping trauma produced a wedge-shaped, highly reproducible lesion involving the parietal cortex and subcortical white matter (Fig. 1A). Grossly, the lesion was characterized by a central cavity encompassed by a zone of hemorrhagic necrosis well delineated from the surrounding tissue. The lesion in the edaravone group was less severe than that in the vehicle group, except for in the low dose (0.75 mg/kg) group, in which the lesion was similar to controls (Fig. 1A). Microscopically, the outline of the hippocampal CA2 and CA3 areas was damaged following TBI (Fig. 1C). The neuronal number in the hippocampal CA3 area shown by Nissl staining was
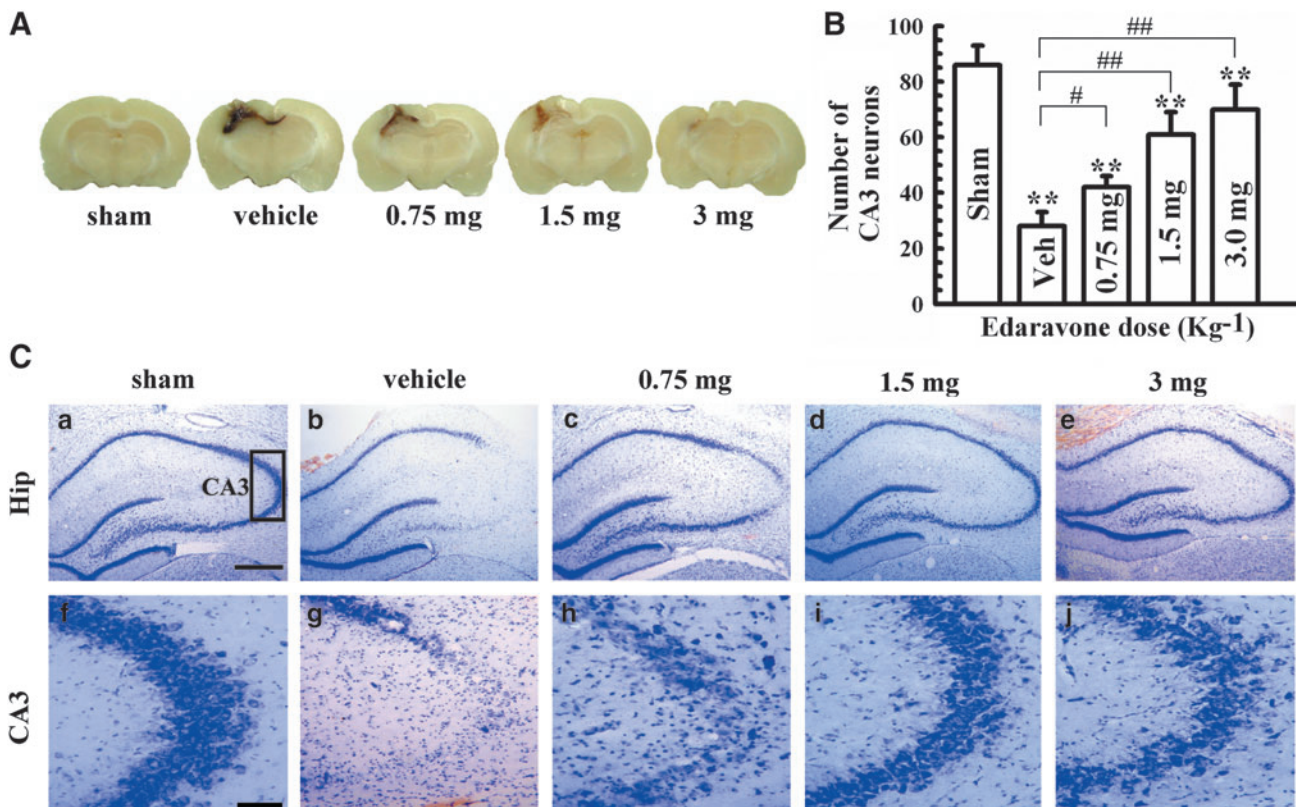

FIG. 1. Dose-dependent neuroprotective effect of edaravone in rats at 72 h after TBI. **(A)** Macroscopic appearance of the focal injury produced by weight-dropping trauma in a coronal section. **(B)** Quantification of the number of neurons in the CA3 area of the right-side hippocampus in the various treatment groups. Quantification was performed as outlined in the Methods section. **(C)** Nissl staining of the right hippocampus in different treatment groups. **(a)**, sham-operated group; **(b)**, vehicle-treated group; **(c–e)**, 0.75, 1.5, 3 mg (kg^{-1}) of edaravone. **(f–j)**, Amplified photographs of the corresponding groups, a-e, respectively. Bars represent mean ± standard deviation. $n = 6$ rats/group for all experiments. CA3, hippocampal cornu amonis 3 area; Hip, hippocampus; Sham, sham-operated group; Veh, vehicle-treated group. **p < 0.01, vs. sham group; # p < 0.05, ## p < 0.01, vs. vehicle group. Scale bar = 0.5 mm in **a–e**, 50 μm in **f–j**. Color image is available online at www.liebertonline.com/neu

reduced greatly after TBI (28.3 ± 4.5). Rats treated with edaravone ($1.5 \, mg/kg$), however, had significantly increased neuronal number (60.8 ± 8.3) compared to the vehicle group (Fig. 1B). There were no differences in CA3 neuronal number between the $1.5 \, mg/kg$ and $3.0 \, mg/kg$ edaravone groups (Fig. 1B). Edaravone at a dose of $1.5 \, mg/kg$ was selected for the following experiments because of its visible efficacy on neuronal number. These data established the proof of principle that edaravone is neuroprotective following TBI. We therefore attempted further examination to more fully characterize the spectrum of edaravone's effects.

Edaravone treatment inhibited oxidative stress

Edaravone functions as a free radical scavenger (Lapchak, 2010). Therefore, we sought to determine if edaravone treatment reduced the presence of free radicals and decreased overall oxidative stress following TBI. To test this, we examined levels of SOD, an enzyme that functions as a superoxide antioxidant, MDA, a reactive aldehyde formed from lipid peroxidation caused by reactive oxygen species (ROS), NO, a byproduct of N-methyl D-aspartate (NMDA) receptor activation that combines with superoxide to form the potent DNA-damaging agent peroxynitrite, and inducible iNOS, an enzyme mainly expressed in macrophages to produce NO and vasodilation following TBI, and shown to be deleterious to brain (Wada et al., 1998). We found in vehicle-treated rats that the activity of SOD in the harvested cortex was significantly decreased, and that the levels of MDA, NO, and iNOS were significantly increased 72 h after TBI (Table 1). Edaravone treatment notably attenuated TBI-induced oxidative stress as formation of MDA and NO was decreased, the activity of iNOS was reduced, and SOD activity increased (Table 1). Cumulatively, these data endorse that edaravone diminishes the degree of oxidative stress as evidenced by multiple measures.

Edaravone treatment suppressed neuronal PCD after TBI

Neuronal PCD is a common phenomenon following TBI, in which neurons surrounding the initial trauma that are not immediately killed die in a delayed and controlled fashion (Greve and Zink, 2009). Therefore, we wanted to see if attenuation of oxidative stress with edaravone had an effect on neuronal PCD. Transmission electron microscopy investigations revealed obvious changes in cellular structure 72 h after TBI. In the sham-operated group, most nuclei appeared normal with an intact nuclear envelope and diffuse chromatin (Fig. 2B). In the vehicle group, irregularity of the nuclear membrane, extended perinuclear margination, and clumping of chromatin of many neurons were observed (Fig. 2B). In contrast, the edaravone ($1.5 \, mg/kg$) group showed only slightly irregular nuclear membranes with a lack of perinuclear edema (Fig. 2B), and no degeneration was observed in small-sized myelinated axons and non-myelinated axons (data not shown).

Another measure of activation of the PCD cascade is via measurement of a zymogen cleaved and activated upon conduction of the mitochondrial or intrinsic PCD cascade, caspase-3. TBI markedly increased activated caspase-3-positive neurons in the parietal cortex in the border of the impact area. In contrast, both immunofluorescence and DAB staining of positive neurons of activated caspase-3 were reduced in the same brain areas by edaravone treatment (Fig. 2C and D). Expression of activated caspase-3 measured by Western blot increased markedly in the cortex harvested at 72 h after TBI compared with sham-operated animals (Fig. 2E and F). Edaravone treatment, however, clearly attenuated caspase-3 activation compared to the vehicle-treated group (Fig. 2E and F). Together, these data indicate that edaravone suppresses delayed neuronal death caused by TBI.

Edaravone suppresses the activation of astrocytes and microglia after TBI

It has been suggested that activation of astroglia may play a role in the pathogenesis of TBI, including contributing to oxidative stress, inflammation, and BBB permeability (Serrano-Perez et al., 2011). We therefore wanted to determine if reduction of oxidative stress via edaravone treatment would suppress astrocyte and microglia activation. We first probed for markers of astrocyte activation: expression of GFAP, vimentin, and S-100. Following TBI there was a dramatic increase in reactive astrocytes determined by increased numbers of astrocytes staining positively for GFAP, vimentin, and S-100 in vehicle-treated rats compared to sham controls (Fig. 3A–D). Astrocytes expressing GFAP also demonstrated a distinct morphology characterized by an enlarged cell body and long intertwined processes (Fig. 3Ab), and were present in the injured cortex, subcortical white matter tracts, and hippocampal CA3 area in vehicle-treated rats (data not shown). Post-traumatic vimentin and S-100 immunoreactivity in astrocytes increased mainly in the perimeter of the cortical lesion, in the subcortical white matter, and in the hippocampus in vehicle-treated rats (data not shown). Consistent with our hypothesis that edaravone's antioxidant effect would suppress reactive astrocytosis, cells expressing markers of astrocyte activation were significantly reduced following TBI (Fig. 3A–D).

Supporting our immunohistochemical data, Western blot analysis of levels GFAP, vimentin, and S-100 expression were also significantly increased in vehicle-treated rats, but not following edaravone treatment (Fig. 3E–G). There were no

TABLE 1. EFFECT OF EDARAVONE ON OXIDATIVE STRESS VARIABLES IN THE IPSILATERAL CORTEX OF RATS AFTER TBI ($N=6$)

Group	SOD (U/mg prot)	MDA (nmol/mg prot)	NO (μmol/g prot)	iNOS (U/mg prot)
Sham	128.11 ± 16.37**	3.15 ± 0.88**	3.64 ± 1.07**	0.15 ± 0.04**
Vehicle	84.85 ± 14.72	5.83 ± 1.25	5.90 ± 1.13	0.43 ± 0.12
Edaravone	108.78 ± 10.71*	3.73 ± 0.76**	4.23 ± 0.70*	0.22 ± 0.05**

$*p < 0.05$, $**p < 0.01$, vs. vehicle. Sham, sham-operated rats.
iNOS, inducible nitric oxide synthase; MDA, malondialdehyde; NO, nitric oxide; SOD, superoxide dismutase.
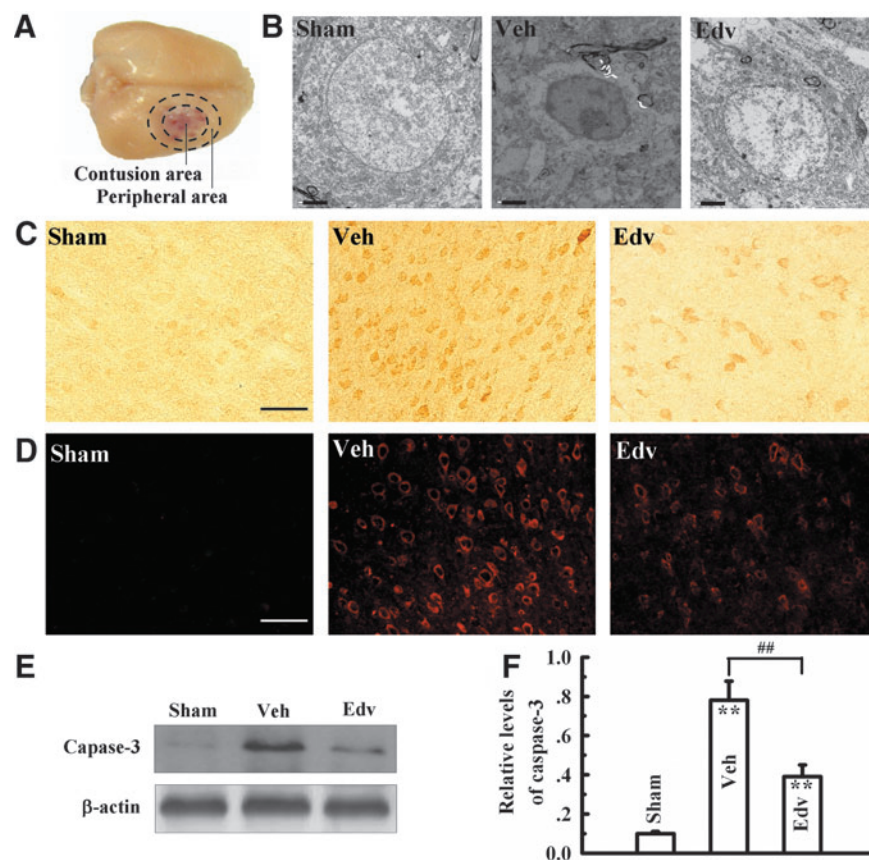
FIG. 2. Neuronal ultrastructural changes in the cerebral cortex and expression of activated caspase-3. **(A)** Schematic representation of the studied region 72 h after weight drop-induced TBI. The region of interest is between the internal and external circles (the pericontusional cortex). **(B)** Ultrastructural configuration of neurons in the sham-operated, vehicle-treated and edaravone-treated rats, respectively. Note the nuclear pyknosis and chromatin condensation in the vehicle-treated rat brain compared to sham and edaravone-treatments. **(C)** Active caspase-3 immunohistochemistry and **(D)** immunofluorescent photographs of active caspase-3 in the cortex surrounding the contusion area that was increased in vehicle-treated rats compared to sham-operated and edaravone-treated rats. **(E)** A representative Western blot of caspase-3 expression in the experimental groups. Caspse-3 expression corresponded to the immunohistochemical and immunofluorescent data. **(F)** Semi-quantification of caspase-3 expression relative to β-actin. Bars represent mean ± standard deviation. Veh, vehicle-treated group; Edv, edaravone-treated group. $n = 4$ rats/group for all experiments. **$p < 0.01$, *vs.* sham group; ##$p < 0.01$, vs. vehicle group. Scale bar = 2 μm in **B**, 50 μm in **C** and **D**. Color image is available online at www.liebertonline.com/neu

statistically significant differences between edaravone-treated rats and sham controls in expression of these proteins.

To identify activated microglia, we performed immunofluorescence labeling for OX42 at 72 h after TBI. OX42 immunoflourescence was markedly increased in TBI brains compared to sham-operated brains. OX42-positive cells displayed hypertrophic morphology indicative of ramified microglia, showing an elongated soma with processes extending from both poles of the cell (Fig. 4A). OX42 labeling in the present study was greater in the brain tissue surrounding the cortical contusion area of the vehicle-treated group, but was reduced greatly after treatment with edaravone (Fig. 4A). Together, these results show that edaravone treatment greatly suppresses astrocyte and microglial activation following TBI.

Edaravone treatment decreased inflammatory reaction

Damage caused by TBI also results in a substantial neuroinflammatory reaction with increases in pro-inflammatory cytokines including IL-1β, IL-6, and TNF-α. Although there is controversy as to whether these cytokines are beneficial or

detrimental following TBI (Laird et al., 2008), we wanted to determine the effect of edaravone treatment on their expression levels. Compared with the sham-operated group, the cortical levels of three pro-inflammatory cytokines, IL-6, IL-1β, and TNF-α were elevated (Fig. 4B–D), and the level of anti-inflammatory cytokine IL-10 was simultaneously reduced in the vehicle-treated group after TBI (Fig. 4E). Edaravone treatment at the effective dose (1.5 mg/kg) significantly lessened the production of TNF-α, IL-6, and IL-1β and concomitantly increased IL-10 to control levels in the brain (Fig. 4B–E). Interestingly, the amounts of inflammatory cytokines were also highly negatively correlated to the levels of SOD, and positively correlated to the amount of MDA (Fig. 4F and G, respectively). This indicates that the antioxidant mechanism of edaravone also acts to decrease neuroinflammation after TBI.

Edaravone decreases cerebral edema and BBB permeability and improves neurological function

The pathogenesis of TBI also involves increased cerebral edema and BBB permeability, possibly because of astrocyte
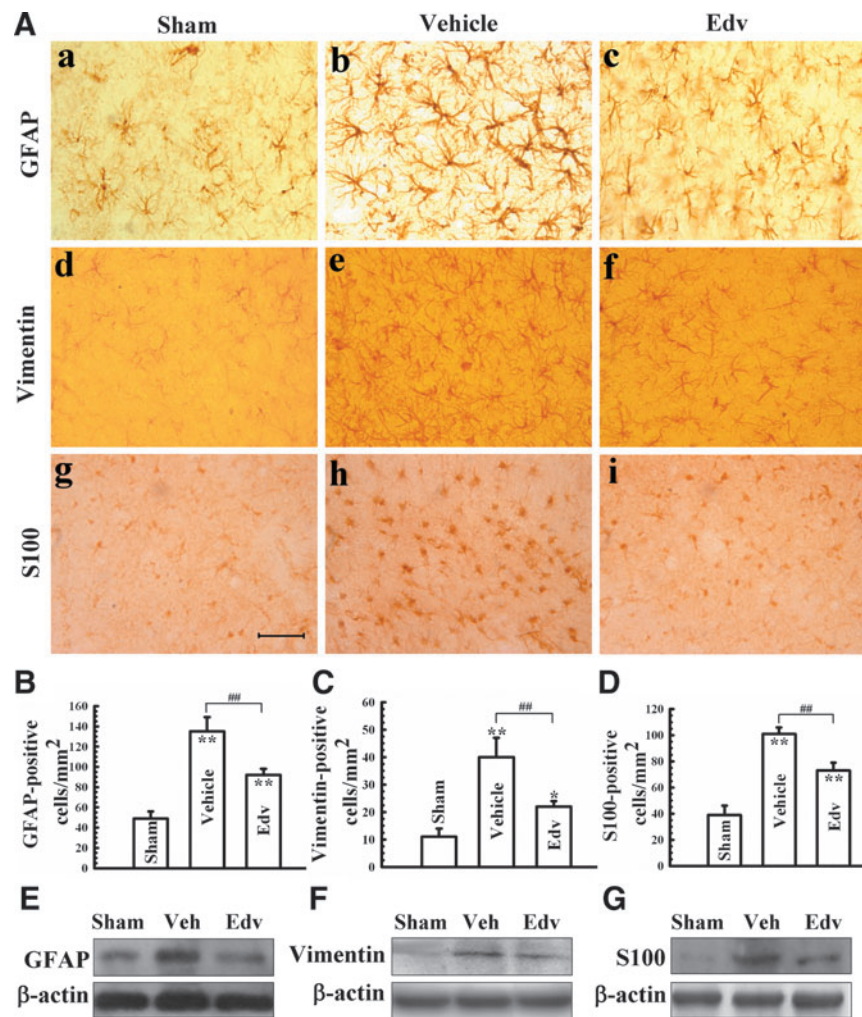
FIG. 3. Inhibition of astrocyte activation by edaravone. **(A)** Representative immunohistochemistry staining of microtubule proteins expressed following astrocyte activation, GFAP **(a–c)**, vimentin **(d–f)**, and S-100 **(g–i)**, in brain tissue surrounding the contusion site are upregulated following TBI in vehicle-treated rats **(b, e, and h)** compared to sham-operated **(a, d, g)**. and edaravone-treated **(c, f, i)** rats. **(B–D)** Quantification of cells positive for GFAP-, vimentin-, and S-100, respectively. **(E–G)** Representative Western blots of GFAP, vimentin, and S-100, respectively with semi-quantification data for each protein relative to β-actin directly underneath the representative blot. Bars represent mean $\pm$ standard deviation. $n = 4$ rats/group for all experiments. $^{*}p < 0.05$, $^{**}p < 0.01$, vs. sham group; $^{\#\#}p < 0.01$, vs. vehicle group. Edv, edaravone-treated group; GFAP, glial fibrillary acidic protein; Veh, Vehicle-treated group; Vim, vimentin. Scale bar $= 50 \mu$m. Color image is available online at www.liebertonline.com/neu

activation or neuroinflammation. Because edaravone treatment markedly diminished these responses to TBI, we wanted to determine if edaravone treatment also decreased formation of edema and BBB permeability. As expected, TBI resulted in increased brain edema and BBB permeability in vehicle-treated rats, as measured by brain water content and Evans blue dye diffusion, respectively (Fig. 5 A and B). Brain water content and BBB permeability increases were prevented by edaravone treatment in a dose-dependent manner compared with the vehicle-treated group (Fig. 5A and B).

The last and perhaps most important aspect of evaluation of a potential therapeutic, in addition to ensuring that the damage caused by TBI is diminished, is to establish that the therapeutic produces neurobehavioral recovery (Vosler and Chen, 2009). Following TBI, there was a pronounced neurological deficit as measured by beam-balancing and prehensile traction tests in vehicle-treated rats compared to sham controls. Treatment

with edaravone significantly improved the neurological score compared to vehicle-treated rats (Fig. 5C). Importantly, the improved neurological score was highly correlated to the increased number of viable CA3 neurons ($r = 0.86$, $p < 0.001$; Fig. 5D). Therefore, our data demonstrate that edaravone treatment results in neurobehavioral protection that is correlated with decreased neuronal loss following TBI.

Discussion

The current data provide further evidence that edaravone is a potential therapeutic for treatment of TBI because of its improvement of multiple measures of cerebral damage. Our data show that probably because of edaravone's antioxidant mechanism, treatment with the pharmacological agent decreases neuronal loss, ROS, PCD, astrocytosis, neuroinflammation, cerebral edema, BBB permeability, and,
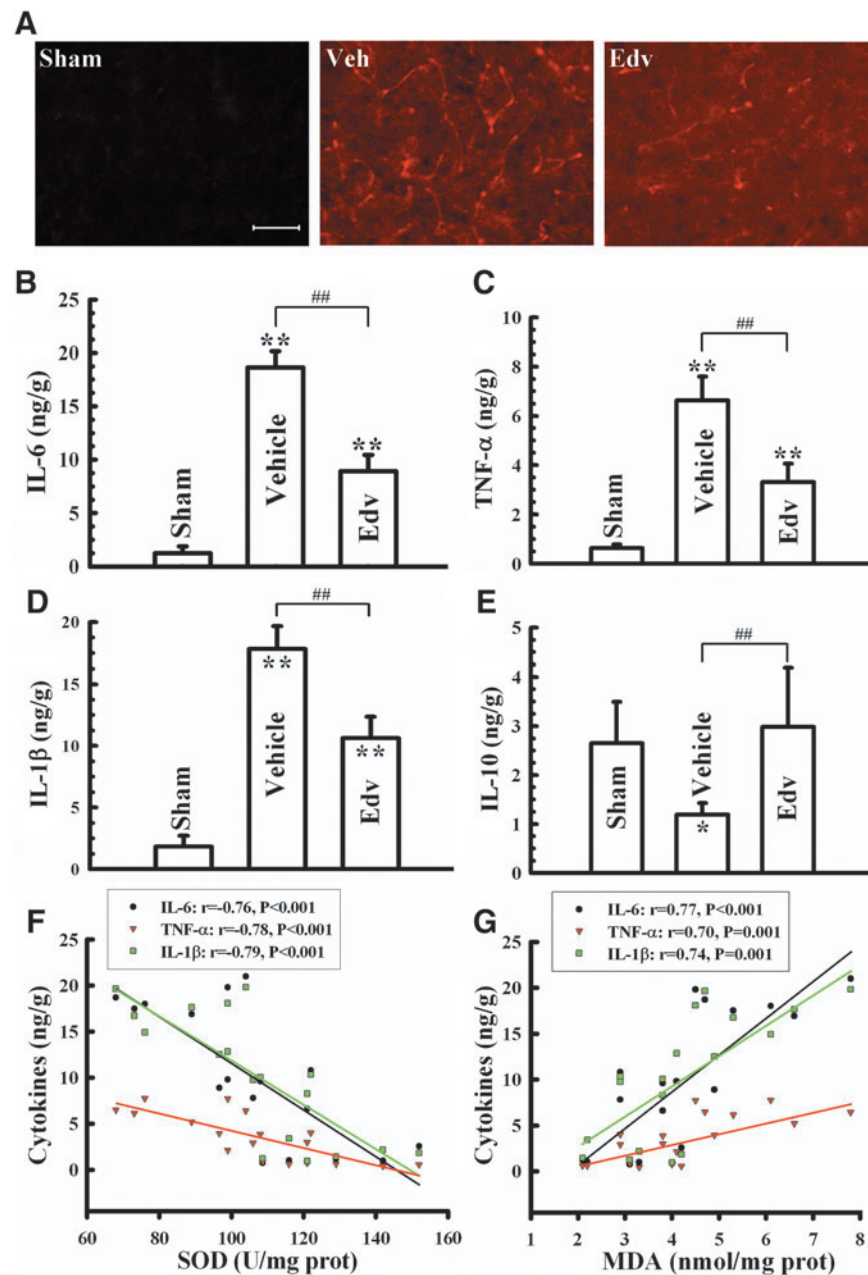
FIG. 4. Effect of edaravone on microglia activation and inflammatory cytokine expression. **(A)** Expression of a microglial-specific protein upregulated following microglial activation, OX42, shows increased immunofluorescence in brain tissue surrounding the contusion site in vehicle-treated rats compared to sham-operated and edaravone-treated rats 72 h following TBI ($n = 4$ rats/group). Expression of the pro-inflammatory cytokines IL-6 **(B)**, TNF-α **(C)**, and IL-1β **(D)** increased following TBI, an effect that was blunted by edaravone treatement. **(E)** In contrast, expression of the anti-inflammatory cytokine IL-10 was decreased in vehicle-treated rats after TBI, but remained at control levels in edaravone-treated rats. Bars represent mean ± standard deviation with $n = 6$ rats/group, and they represent the amount of cytokine in nanograms relative to grams of protein in the sample as measured by ELISA. **(F)** The levels of pro-inflammatory cytokines IL-1β, IL-6, and TNF-α were strongly inversely correlated to the amount of the antioxidant SOD measured in the same rats as depicted by the line graph. **(G)** Levels of the byproduct of lipid peroxidation MDA were accordingly highly positively correlated with the levels of the pro-inflammatory cytokines measured. Data points in line graphs represent the levels of the inflammatory cytokines and either SOD or MDA taken from individual rats ($n = 18$ rats). Edv, edaravone-treated group; ELISA, enzyme-linked immunosorbent assay; IL-1β, −6, and −10, interleukin-1β, −6, and −10; MDA, malondialdehyde; SOD, superoxide dismutase; TNF-α, tumor necrosis factor- α; Veh, vehicle-treated group. $*p < 0.05$, $**p < 0.01$, vs. sham group; $^{\#\#}p < 0.01$, vs. vehicle group. Scale bar = 50 μm. Color image is available online at www.liebertonline.com/neu
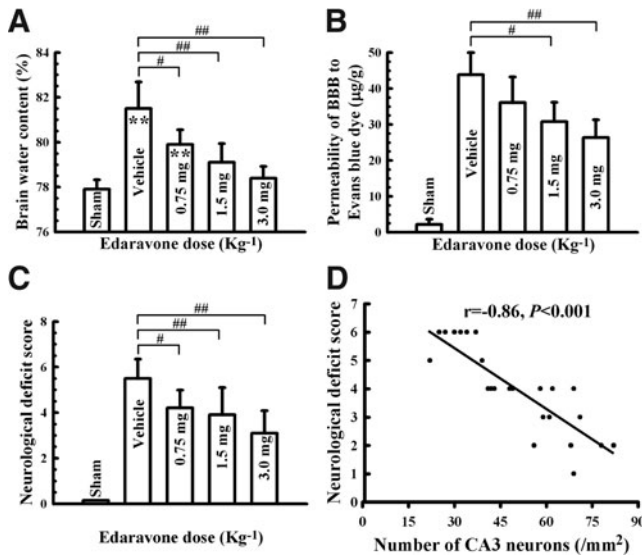
FIG. 5. Decreases in cerebral edema, BBB permeability and improved neurological deficit following edaravone treatment. **(A)** Cerebral edema as measured by brain water content ($n = 6$ rats/group), calculated by $100 \times$ (wet weight − dry weight)/wet weight, was significantly increased in vehicle-treated rats following TBI. This finding was decreased in a dose-dependent manner with edaravone treatement. **(B)** Similarly, BBB permeability, determined by penetration of Evans blue dye into the brain tissue across the **BBB** was also increased in vehicle-treated rats following TBI, but abrogated in a dose-dependent manner with edaravone treatment ($n = 6$ rats/group). **(C)** Neurological deficit scores were calculated based on the rats' performance on the beam-balancing and prehensile traction tests following their respective treatment. Rats treated with edaravone showed a significantly decreased neurological deficit compared to vehicle-treated rats 72 h after TBI ($n = 10$ rats/group). **(D)** The number of CA3 neurons was highly and inversely correlated to functional deficits evaluated by neurological deficit scores as depicted by the line graph. Bars represent mean ± standard deviation. CA3, hippocampal cornu amonis 3 area. Hip, hippocampus; Sham, sham-operated group. $^{#}p < 0.05$, $^{##}p < 0.01$, vs. vehicle group.

importantly, it also results in improved neurological function following TBI. Our data also demonstrate that the presence of ROS is correlated to neuroinflammatory markers, and improved neurological function is highly correlated to decreased hippocampal CA3 cell loss. Collectively, these experiments provide clear experimental data to validate the efficacy of edaravone treatment on TBI. Although a few investigators have reported that early use of edaravone had beneficial effects on TBI (Dohi et al., 2006, 2007; Itoh et al., 2010), the dose-dependent effects of edaravone on the aforementioned parameters have rarely been studied, and the present study provides more comprehensive evidence.

Oxidative stress is considered to play a central role as one of the mechanisms underlying secondary brain damage following TBI (Petronilho et al., 2010). Compelling evidence supports a role for antioxidant strategies aimed at decreasing post-traumatic neurological deficits, cerebral edema, and brain lesion volume induced by oxidative stress (Clausen et al., 2008; Eghwrudjakpor and Allison, 2010; Hall et al.,

2010). Therefore, we investigated the effect of edaravone on oxidative stress after TBI. Our results demonstrate that systemic administration of edaravone in a rat model of TBI not only decreased the formation of MDA and NO and the activity of iNOS, but also increased the activity of the superoxide antioxidant SOD. These results are consistent with previously published reports (Dohi et al., 2006, 2007). It has been reported that edaravone inhibits both nonenzymatic lipid peroxidation and the lipoxygenase pathway (Watanabe et al., 1988), and it has potent antioxidant effects against ischemia and reperfusion-induced vascular endothelial cell injury, delayed neuronal death, brain edema, and concomitant neurological deficits (Yoshida et al., 2006). The majority of these findings were reproduced in the current study.

It should be noted that the MDA assay is not an ideal assay for the detection of lipid peroxidation, as MDA is both produced directly from free radical attack on fatty acids, and formed as a byproduct of lipoxygenase processing of arachidonic acid (Griesser et al., 2009). Therefore, the levels of MDA are not a completely specific indicator of oxidative stress. Total oxidative stress under vehicle-treated conditions may thus overestimate lipid peroxidation because of oxidative stress. Edaravone, however, is known to block both the formation of free radicals and the conversion of arachidonic acid by inhibiting lipoxygenase (Watanabe et al., 1988). The reduction of MDA in edaravone-treated rats is caused by inhibition of both pathways, and our results indicate that edaravone treatment decreased MDA production to sham-treated levels (Table 1). Therefore, measurement of MDA is valid in our study. To avoid this confounder, future studies will also measure the production of the more specific aldehyde produced during lipid peroxidation, 4-hydroxynonenal, via antibody-directed methods (Spickett et al., 2010).

The brain is particularly vulnerable to oxidative stress, as it contains low levels of antioxidant enzymes and high concentrations of iron that catalyze the production of free radicals, and is rich in unsaturated fatty acids that are targets for lipid peroxidation (Margaill et al., 2005). After brain damage caused by trauma, physiological systems involved in the removal of excess free radicals, such as SOD, are impaired, and the formation of free radicals is increased (Greve and Zink, 2009). Elevation of free radicals damages all cellular components, including DNA, lipids, and proteins, leading to injuries of neurons, glial cells, nerve fibers, and blood vessels. Oxidative stress damages the BBB, leading to vasogenic brain edema, neuronal degeneration, and deteriorating neurological function, probably caused by the accelerated formation of several ROS including superoxide, hydroxyl radical (OH), NO (Dohi et al., 2006; Eghwrudjakpor and Allison, 2010; Merenda et al., 2008).

NO is generated by iNOS, an enzyme expressed in macrophages, neutrophils, and microglia, following immunological inflammatory stimuli whose activation is thought to be detrimental following TBI (Wada et al., 1998). Increased production of NO may therefore also contribute to late-stage tissue injury (Yoshida et al., 2006). We found activation of microglia after TBI in the present study, which was markedly inhibited by edaravone. This inhibition likely occurred because of the antioxidant effect of edaravone.

Another pathway known to be activated in response to TBI is cellular and humoral inflammation (Lu et al., 2009; Pearse and Jarnagin, 2010; Ziebell and Morganti-Kossmann, 2010). In

this study, we found that the expression of pro-inflammatory cytokines TNF-α, IL-1β, and IL-6 was highly upregulated after TBI; the anti-inflammatory cytokine IL-10 was down-regulated; and the number of microglia was increased. These changes might promote the development of neuroinflammation after brain trauma.

Neuroinflammation within injured brain has long been considered to intensify the damage sustained following TBI (Lu et al., 2009; Ziebell and Morganti-Kossmann, 2010). An imbalance between pro- and anti-inflammatory actions has been hypothesized to cause pathological responses. Recent studies suggest that pro-inflammatory cytokines (e.g., TNF-α) can antagonize cell survival cascades (e.g., PI3-kinase) initiated by anti-inflammatory cytokines (IL-10) (Gottesfeld et al., 2002). At high levels of pro-inflammatory cytokines, additional biochemical cascades (e.g., caspase cascades) are activated, leading to cell death (Venters et al., 2000).

Following TBI, the excessive release of IL-1β and TNF-α is a major cause of cerebral edema, which, in turn, can cause permanent neuronal loss and cognitive deficits in laboratory rats (Ziebell and Morganti-Kossmann, 2010). IL-6 has been reported to be highly elevated in cerebrospinal fluid (CSF) and to a lesser extent in serum; serum concentrations were associated with increased acute phase proteins (C-reactive protein, fibrinogen, and α1-antitrypsin) and with severe BBB dysfunction (Kossmann et al., 1995). Moreover, inflammatory cytokines can be released by activated microglia (Stoll and Jander, 1999). Failed microglial engagement caused by excessive or sustained activation resulting from TBI could significantly contribute to acute and chronic neuropathologies (Hanisch, 2002). Dysregulation of microglial cytokine production could result in direct neurotoxicity, as well as disturbing neural cell functions, as they are sensitive to cytokine signaling (Hanisch, 2002).

In a mouse transient focal ischemia model, it has been found that edaravone afforded a late anti-inflammatory effect through inhibition of the inflammatory pathway of microglial activation and subsequent reduction of iNOS activity, while it exerted an early neuroprotective effect through suppression of the accumulation of lipid peroxidative products and oxidative DNA damage (Zhang et al., 2005). In the present study, edaravone treatment similarly reduced TBI-induced production of pro-inflammatory cytokines, elevated the content of anti-inflammatory cytokines, and suppressed the hyperactive microglia, thereby potentially contributing to inhibition of neuroinflammation.

TBI triggers a cascade of events that may contribute to secondary brain damage, among which is reactive astrocytosis (Laird et al., 2008). In the short term, reactive astrocytes augment pro-inflammatory responses, permeability of the BBB, and cerebral edema, thus worsening neurological outcomes (Tacconi, 1998; Vajtr et al., 2009). In the long term, they form glial scars that are believed to severely restrict axonal regeneration and synaptic plasticity, thus obstructing brain repair after TBI (Laird et al., 2008; Sofroniew, 2009). Reactive astrocytes show an increase in the expression of two intermediate filaments, GFAP and vimentin, found in mature and immature astrocytes, respectively (Hill et al., 1996). The S-100 protein is another marker of cytoskeletal changes that occur in all reactive astrocytes following TBI (Hill et al., 1996). In the present study, we found a significant increase in reactive astrocytes in brain tissue surrounding the primary injury by cell counting of GFAP-, S100-, and vimentin-positive astrocyte cells. Edaravone treatment notably reduced the reactive astrocytes, showing novel evidence of benefits afforded by edaravone in the treatment of TBI. These results suggest that modulation of responsive astrocyte activation might be a potential therapeutic target for TBI.

Alternatively, reactive astrocytosis has also been shown to be beneficial following acute neuronal injury resulting from TBI. Two current hypotheses regarding the benefit of reactive astrocytosis are that it limits tissue damage caused by reduction of inflammatory markers and that it can stimulate brain tissue regeneration (for review, see Laird et al., 2008). Important issues regarding the discrepancy between the roles of reactive astrocytosis include type of injury, severity of injury, and the method of neuroprotection used in the various studies.

Concerning the present study, it is likely that edaravone's free-radical scavenging mechanism may limit the sequelae causing reactive astrocytosis, that is, ROS formation. Indeed, our results indicate that diminished ROS was associated with decreased presence of reactive astrocytes, and highly correlated with decreased neuroinflammation (Fig. 4F and G). The benefits of reactive astrocytosis may not have been appreciated in this article because the stimulus causing reactive astrocytosis, ROS, was attenuated.

Clinically, uncertainties remain concerning the efficacy of edaravone for the treatment of acute ischemic stroke patients, and additional clinical studies are necessary (Lapchak, 2010). Research on the efficacy of edaravone in the treatment of TBI in both animal models and human patients has recently been started, and the present study provides new evidence to support edaravone's use in clinical trials for the treatment of TBI patients. Furthermore, no apparent adverse effects have been reported in treating stroke patients clinically (Lapchak, 2010). Therefore, edaravone may be a novel candidate for neuroprotection in the clinical treatment of TBI.

Conclusion

In conclusion, edaravone treatment reduced brain edema, BBB permeability, and neuronal death, and improved neurological function, suggesting that systemic administration of the synthetic free-radical scavenger edaravone is neuroprotective in a rat model of TBI. In addition, edaravone diminished the level of oxidative stress-related byproducts and inflammation-related cytokines in the brain, reinforcing the importance of oxidative stress and inflammatory reaction in the pathogenesis of secondary neuronal injury following TBI. Moreover, edaravone inhibited reactive astrocytes as well as hyperactive microglia, indicating that modulation of responsive microglial activation might be a potential therapeutic target.

Acknowledgments

Author Disclosure Statement

No conflicting financial interests exist.

References

Aarabi, B., and Simard, J. M. (2009). Traumatic brain injury. Curr. Opin. Crit. Care 15, 548–553.

Besson, V. C. (2009). Drug targets for traumatic brain injury from poly(ADP-ribose)polymerase pathway modulation. Br J Pharmacol 157, 695–704.

Chew, E., and Zafonte, R. D. (2009). Pharmacological management of neurobehavioral disorders following traumatic brain injury–a state-of-the-art review. J. Rehabil. Res. Dev. 46, 851–879.

Chua, K. S., Ng, Y. S., Yap, S. G., and Bok, C. W. (2007). A brief review of traumatic brain injury rehabilitation. Ann. Acad. Med. Singapore 36, 31–42.

Clausen, F., Lundqvist, H., Ekmark, S., Lewen, A., Ebendal, T., and Hillered, L. (2004). Oxygen free radical-dependent activation of extracellular signal-regulated kinase mediates apoptosis-like cell death after traumatic brain injury. J. Neurotrauma 21, 1168–1182.

Clausen, F., Marklund, N., Lewen, A., and Hillered, L. (2008). The nitrone free radical scavenger NXY-059 is neuroprotective when administered after traumatic brain injury in the rat. J. Neurotrauma 25, 1449–1457.

Dohi, K., Satoh, K., Mihara, Y., Nakamura, S., Miyake, Y., Ohtaki, H., Nakamachi, T., Yoshikawa, T., Shioda, S., and Aruga, T. (2006). Alkoxyl radical-scavenging activity of edaravone in patients with traumatic brain injury. J. Neurotrauma 23, 1591–1599.

Dohi, K., Satoh, K., Nakamachi, T., Yofu, S., Hiratsuka, K., Nakamura, S., Ohtaki, H., Yoshikawa, T., Shioda, S., and Aruga, T. (2007). Does edaravone (MCI- 186) act as an antioxidant and a neuroprotector in experimental traumatic brain injury? Antioxid. Redox Signal. 9, 281–287.

Eghwrudjakpor, P. O., and Allison, A. B. (2010). Oxidative stress following traumatic brain injury: enhancement of endogenous antioxidant defense systems and the promise of improved outcome. Niger. J. Med. 19, 14–21.

Gilgun–Sherki, Y., Rosenbaum, Z., Melamed, E., and Offen, D. (2002). Antioxidant therapy in acute central nervous system injury: current state. Pharmacol. Rev. 54, 271–284.

Gottesfeld, Z., Moore, A. N., and Dash, P. K. (2002). Acute ethanol intake attenuates inflammatory cytokines after brain injury in rats: a possible role for corticosterone. J. Neurotrauma 19, 317–326.

Greve, M. W., and Zink, B. J. (2009). Pathophysiology of traumatic brain injury. Mt. Sinai J. Med. 76, 97–104.

Griesser, M., Boeglin, W.E., Suzuki, T., and Schneider, C. (2009). Convergence of the 5-LOX and COX-2 pathways: heme-catalyzed cleavage of the 5S-HETE-derived di-endoperoxide into aldehyde fragments. J. Lipid Res. 50, 2455–2462.

Hall, E. D., Vaishnav, R. A., and Mustafa, A. G. (2010). Antioxidant therapies for traumatic brain injury. Neurotherapeutics 7, 51–61.

Hanisch, U. K. (2002). Microglia as a source and target of cytokines. Glia 40, 140–155.

Hill, S. J., Barbarese, E., and McIntosh, T. K. (1996). Regional heterogeneity in the response of astrocytes following traumatic brain injury in the adult rat. J. Neuropathol. Exp. Neurol. 55, 1221–1229.

Itoh, T., Satou, T., Nishida, S., Tsubaki, M., Imano, M., Hashimoto, S., and Ito, H. (2010). Edaravone protects against apoptotic neuronal cell death and improves cerebral function after traumatic brain injury in rats. Neurochem. Res. 35, 348–355.

Kikuchi, K., Kawahara, K., Miyagi, N., Uchikado, H., Kuramoto, T., Morimoto, Y., Tancharoen, S., Miura, N., Takenouchi, K., Oyama, Y., Shrestha, B., Matsuda, F., Yoshida, Y., Arimura, S., Mera, K., Tada, K., Yoshinaga, N., Maenosono, R., Ohno, Y., Hashiguchi, T., Maruyama, I., and Shigemori, M. (2010). Edaravone: a new therapeutic approach for the treatment of acute stroke. Med. Hypotheses 75, 583–585.

Kossmann, T., Hans, V. H., Imhof, H. G., Stocker, R., Grob, P., Trentz, O., and Morganti–Kossmann, C. (1995). Intrathecal and serum interleukin-6 and the acute-phase response in patients with severe traumatic brain injuries Shock 4, 311–317.

Laird, M. D., Vender, J. R., and Dhandapani, K. M. (2008). Opposing roles for reactive astrocytes following traumatic brain injury. Neurosignals 16, 154–164.

Lapchak, P. A. (2010). A critical assessment of edaravone acute ischemic stroke efficacy trials: is edaravone an effective neuroprotective therapy? Expert Opin. Pharmacother. 11, 1753–1763.

Lu, J., Goh, S. J., Tng, P. Y., Deng, Y. Y., Ling, E. A., and Moochhala, S. (2009). Systemic inflammatory response following acute traumatic brain injury. Front. Biosci. 14, 3795–3813.

Maas, A. I., Stocchetti, N., and Bullock, R. (2008). Moderate and severe traumatic brain injury in adults. Lancet Neurol. 7, 728–741.

Margaill, I., Plotkine, M., and Lerouet, D. (2005). Antioxidant strategies in the treatment of stroke. Free Radic. Biol. Med. 39, 429–443.

Merenda, A., Gugliotta, M., Holloway, R., Levasseur, J. E., Alessandri, B., Sun, D., and Bullock, M. R. (2008). Validation of brain extracellular glycerol as an indicator of cellular membrane damage due to free radical activity after traumatic brain injury. J. Neurotrauma 25, 527–537.

Naritomi, H., Moriwaki, H., Metoki, N., Nishimura, H., Higashi, Y., Yamamoto, Y., Yuasa, H., Oe, H., Tanaka, K., Saito, K., Terayama, Y., Oda, T., Tanahashi, N., and Kondo, H. (2010). Effects of edaravone on muscle atrophy and locomotor function in patients with ischemic stroke: a randomized controlled pilot study. Drugs R D 10, 155–163.

Pearse, D., and Jarnagin, K. (2010). Abating progressive tissue injury and preserving function after CNS trauma: The role of inflammation modulatory therapies. Curr. Opin. Investig. Drugs 11, 1207–1210.

Petronilho, F., Feier, G., de Souza, B., Guglielmi, C., Constantino, L. S., Walz, R., Quevedo, J., and Dal-Pizzol, F. (2010). Oxidative stress in brain according to traumatic brain injury intensity. J. Surg. Res. 164, 316–320.

Regan-Shaw, S., Nihal, M., and Ahmad, N. (2008). Dose translation from animal to human studies revisited. FASEB J. 22, 59–61.

Serrano-Perez, M. C., Martin, E. D., Vaquero, C. F., Azcoitia, I., Calvo, S., Cano, E., and Tranque, P. (2011). Response of transcription factor NFATc3 to excitotoxic and traumatic brain insults: identification of a subpopulation of reactive astrocytes. Glia 59, 94–107.

Shlosberg, D., Benifla, M., Kaufer, D., and Friedman, A. (2010). Blood–brain barrier breakdown as a therapeutic target in traumatic brain injury. Nat. Rev. Neurol. 6, 393–403.

Sofroniew, M. V. (2009). Molecular dissection of reactive astrogliosis and glial scar formation. Trends Neurosci. 32, 638–647.

Spickett, C.M., Wiswedel, I., Siems, W., Zarkovic, K., and Zarkovic, N. (2010). Advanced in methods for the determination of biologically relevant lipid peroxidation products. Free Radic. Res. 44, 1172–1202.

Stoica, B. A., and Faden, A. I. (2010). Cell death mechanisms and modulation in traumatic brain injury. Neurotherapeutics 7, 3–12.

Stoll, G., and Jander, S. (1999). The role of microglia and macrophages in the pathophysiology of the CNS. Prog. Neurobiol. 58, 233–247.

Tacconi, M. T. (1998). Neuronal death: is there a role for astrocytes? Neurochem. Res. 23, 759–765.

Vajtr, D., Benada, O., Kukacka, J., Prusa, R., Houstava, L., Toupalik, P., and Kizek, R. (2009). Correlation of ultrastructural changes of endothelial cells and astrocytes occurring during blood brain barrier damage after traumatic brain injury with biochemical markers of BBB leakage and inflammatory response. Physiol. Res. 58, 263–268.

Venters, H. D., Dantzer, R., and Kelley, K. W. (2000). A new concept in neurodegeneration: TNFalpha is a silencer of survival signals. Trends Neurosci. 23, 175–180.

Vosler, P. S., and Chen, J. (2009). Potential molecular targets for translational stroke research. Stroke 40, S119–120.

Vosler, P. S., Sun, D., Wang, S., Gao, Y., Kintner, D. B., Signore, A. P., Cao, G., and Chen, J. (2009). Calcium dysregulation induces apoptosis–inducing factor release: cross-talk between PARP-1- and calpain-signaling pathways. Exp. Neurol. 218, 213–220.

Wada, K., Chatzipanteli, K., Kraydieh, S., Busto, R., and Dietrich, W. D. (1998). Inducible nitric oxide synthase expression after traumatic brain injury and neuroprotection with aminoguanidine treatment in rats. Neurosurgery 43, 1427–1436.

Wang, G. H., Zhang, X. G., Jiang, Z. L., Li, X., Peng, L. L., Li, Y. C., and Wang, Y. (2010). Neuroprotective effects of hyperbaric oxygen treatment on traumatic brain injury in the rat. J. Neurotrauma 27, 1733–1743.

Watanabe, T., Morita, I., Nishi, H., Murota, S. (1988). Preventive effect of MCI-186 on 15-HPETE induced vascular endothelial cell injury in vitro. Prostaglandins Leukot. Essent. Fatty Acids 33, 81–87.

Yoshida, H., Yanai, H., Namiki, Y., Fukatsu–Sasaki, K., Furutani, N., and Tada, N. (2006). Neuroprotective effects of edaravone: a novel free radical scavenger in cerebrovascular injury. CNS Drug Rev. 12, 9–20.

Zhang, N., Komine–Kobayashi, M., Tanaka, R., Liu, M., Mizuno, Y., and Urabe, T. (2005). Edaravone reduces early accumulation of oxidative products and sequential inflammatory responses after transient focal ischemia in mice brain. Stroke 36, 2220–2225.

Ziebell, J. M., and Morganti–Kossmann, M. C. (2010). Involvement of pro- and anti-inflammatory cytokines and chemokines in the pathophysiology of traumatic brain injury. Neurotherapeutics 7, 22–30.

Address correspondence to:
Jun Chen, M.D., Ph.D.
Department of Neurology
University of Pittsburgh School of Medicine
Pittsburgh, PA 15213

E-mail: chenj2@upmc.edu

or

Zheng-Lin Jiang, M.D., Ph.D.
Department of Neuropharmacology
Institute of Nautical Medicine
Nantong University
Jiangsu, 226001
China

E-mail: jiangzl@ntu.edu.cn